Hong, Hao; Wu, Chunchun; Zhao, Zixun; Zuo, Yonggang; Wang, Jinhuan; Liu, Can; Zhang, Jin; Wang, Fangfang; Feng, Jiangang; Shen, Huaibin; Yin, Jianbo; Wu, Yuchen; Zhao, Yun; Liu, Kehai; Gao, Peng; Meng, Sheng; Wu, Shiwei; Sun, Zhipei; Liu, Kaihui; Xiong, Jie

Giant enhancement of optical nonlinearity in two-dimensional materials by multiphoton-excitation resonance energy transfer from quantum dots

Published in:
Nature Photonics

DOI:
10.1038/s41566-021-00801-2

Published: 01/07/2021

Document Version
Peer-reviewed accepted author manuscript, also known as Final accepted manuscript or Post-print

Please cite the original version:
Hong, H., Wu, C., Zhao, Z., Zuo, Y., Wang, J., Liu, C., Zhang, J., Wang, F., Feng, J., Shen, H., Yin, J., Wu, Y., Zhao, Y., Liu, K., Gao, P., Meng, S., Wu, S., Sun, Z., Liu, K., & Xiong, J. (2021). Giant enhancement of optical nonlinearity in two-dimensional materials by multiphoton-excitation resonance energy transfer from quantum dots. *Nature Photonics*, *15*(7), 510-515. https://doi.org/10.1038/s41566-021-00801-2

Giant enhancement of optical nonlinearity in two-dimensional materials by multiphoton-excitation resonance energy transfer from quantum dots

Hao Hong[1,2#], Chunchun Wu[1,2#], Zixun Zhao[2], Yonggang Zuo[3], Jinhuan Wang[2,4], Can Liu[2], Jin Zhang[3], Fangfang Wang[5], Jiangang Feng[6], Huaibin Shen[5], Jianbo Yin[7], Yuchen Wu[6], Yun Zhao[4], Kehai Liu[8], Peng Gao[2,9], Sheng Meng[3], Shiwei Wu[10], Zhipei Sun[11], Kaihui Liu[2]* and Jie Xiong[1]*

[1] State Key Laboratory of Electronic Thin Films and Integrated Devices, University of Electronic Science and Technology of China, Chengdu 610054, China

[2] State Key Lab for Mesoscopic Physics and Frontiers Science Center for Nano-optoelectronics, Collaborative Innovation Center of Quantum Matter, School of Physics, Peking University, Beijing 100871, China

[3] Institute of Physics, Chinese Academy of Sciences, Beijing 100080, China

[4] School of Chemistry and Chemical Engineering, Beijing Institute of Technology, Beijing 100081, China

[5] Key Laboratory for Special Functional Materials of Ministry of Education, Henan University, Kaifeng 475004, China.

[6] Technical Institute of Physics and Chemistry, Chinese Academy of Sciences, Beijing 100190, China

[7] Beijing Graphene Institute (BGI), Beijing, China

[8] Songshan Lake Materials Laboratory, Institute of Physics, Chinese Academy of Sciences, Guangdong 523808, China

[9] International Center for Quantum Materials, Electron Microscopy Laboratory, School of Physics, Peking University, Beijing 100871, China

[10] State Key Laboratory of Surface Physics and Department of Physics, Fudan University, Shanghai 200433, China

[11] Department of Electronics and Nanoengineering and QTF Centre of Excellence, Aalto University, Aalto, Finland

# These authors contributed equally to this work

* Correspondence: jiexiong@uestc.edu.cn; khliu@pku.edu.cn

Strong quantum confinement in colloidal quantum dots (QD) endows an outstanding ability in engineering their optical band gap by simply changing their physical size. Such facile spectral tunability, together with near-unity photoluminescence (PL) quantum yield, long-lived carrier lifetime and easy solution processing have led to plentiful photonic and optoelectronic applications of QD ranging from lasers, displays, photodetectors to solar cells[1-9]. However, these applications mainly utilize the linear optical properties of QD and their great potentials in the broad nonlinear optical regimes are still waiting for full exploration[10-12]. Here, we demonstrate that a simple coating of a sub-200 nm-thick QD film on two-dimensional (2D) materials can significantly enhance their nonlinear optical responses by more than three orders of magnitude. This giant enhancement is found to be quite universal in either nonlinear harmonic orders (2^{th}, 3^{th} and 4^{th}) or 2D forms (conducting, semiconducting and insulating atomic monolayers, or thin molecular films). Systematic experimental results further indicate a nontrivial mechanism of multiphoton-excitation resonance energy transfer, where the QD directly deliver their strongly absorbed multiphoton energy to the adjacent 2D materials by a remote dipole-dipole coupling. The transfer efficiency is sufficiently high (~95%), due to the unique advantage of nearly perfect spectral overlap between nonlinear absorption in QD and frequency harmonic generation in two-dimensional materials. Our findings should expand the QD applications with many exciting options beyond linear optics, such as nonlinear optical signal processing, multiphoton imaging and ultracompact nonlinear optical elements.

Nonlinear optics is a fundamental building block of modern optics and lies at the core of many classical and quantum technologies. The introduction of nonlinear optics into 2D materials provides a powerful tool for the study of novel physics in two dimensions[13-16] and expands the versatility of nano-photonic applications, including nonlinear optical modulators, frequency combs and nanolasers[17-19]. Due to the enhanced electronic correlations and large transition dipole matrix elements, 2D materials express especially strong optical nonlinearity at a normalized atomic thickness (e.g., MoS_2 has typical second-order susceptibility $\chi^{(2)}$ of ~10 nm/V at ~800 nm excitation, three orders larger than BBO crystal)[20]. However, their absolute light-matter

interactions are actually too weak (e.g., MoS_2 has second harmonic conversion efficiency of ~10^{-7} only at 10 GW/cm^2 laser pump) to perform any practical applications, mainly due to the reduced interaction length and the lack of phase matching. Previously, many efforts have been devoted to enhancing the optical nonlinearity of 2D materials through the exploitation of electric field, doping or strain, but the enhancement is typically limited within 10s folds only[21-25]. Plasmonic nanocavities, waveguides and metamaterials hold promise for several orders of optical nonlinearity enhancement [26-29], while the local hot spot of electric field sacrifices the spatial homogeneity in a large area.

One plausible way to gain homogeneous enhancement of optical responses in 2D systems is by the massive energy transfer from adjacent photoactive medium[30-32]. Benefitting from the admirable optical properties, such as ultrahigh absorption, near-unity PL quantum yield and nanosecond-scale long-lived photocarrier lifetime, QD are considered to be promising photon energy storage materials and have been successfully used in the linear optical regime as light detection, harvesting and emitter. While for realizing giant nonlinear optical response enhancement in two dimensions by energy transfer, QD have their special advantages serving as photoactive medium. **(*i*)** QD have strong multiphoton nonlinear absorption but silence of frequency harmonic responses, which are ideal candidates for multiphoton energy storage[11]. **(*ii*)** Driven by the long-range dipole-dipole electromagnetic interaction instead of interlayer electronic coupling only, in principle these stored energies in QD can transfer remotely, rapidly and efficiently to the adjacent materials[33-37]. **(*iii*)** The selection rules of photoexcited energy transfer are believed to be weakened in QD due to relaxed momentum matching at zero dimension[38]. Nevertheless, giant nonlinear optical response enhancement in two dimensions with the assistance of energy transfer has not been realized yet. In this work, we demonstrate that the simple coating of sub-200 nm-thick QD films on 2D systems, ranging from atomic layered graphene, molybdenum disulfide (MoS_2) and hexagonal boron nitride (hBN) to 4-dimethylamino-4′-nitrostilbene (DANS) molecular films, can significantly enhance their nonlinear optical responses (2th, 3th and 4th harmonic generation) by up to three orders of magnitude, through a unique mechanism of multiphoton-excitation resonance energy transfer by a high-efficiency remote dipole-dipole coupling.

In our experiments, the hybrid of QD/MoS_2 was fabricated by spin-coating CdSe/ZnS QD on MoS_2 monolayer (Fig. 1a) (See Methods for fabrication details). Under excitation at frequency ω, the second-order susceptibility $\chi^{2\omega}$ gives nonlinear polarization $p^{2\omega} = \varepsilon_0 \chi^{2\omega} E^{\omega} E^{\omega}$, where ε_0 is the permittivity of free space and E^{ω} is the incident electric field. Here under 820 nm femtosecond pulsed laser excitation, MoS_2 monolayer presents a sharp peak at 410 nm as expected for its second harmonic generation (SHG) (Fig. 1b). This SHG intensity in MoS_2 is quite weak with a conversion efficiency of only ~4×10^{-7} (under fundamental pump peak intensity of 20 GW/cm^2). While after QD film coating (the thickness of ~150 nm is used for all the MoS_2 experiments if not specified), the SHG in the hybrid is dramatically enhanced to a conversion efficiency up to ~6×10^{-4}, with ~1500 times enhancement to pristine MoS_2. Since pristine QD films have no observable SHG signal (Fig. 1b) under our experiment condition, the strong SHG response in the hybrid can only be attributed to the enhanced SHG of MoS_2 with adjacent QD. This conclusion can also be directly drawn from the polarization-dependent SHG measurements, where characteristic six-fold anisotropic patterns with the same direction are observed in MoS_2 before and after QD coating (Fig. 1c). As SHG represents the conversion of two photons into one photon, a square dependence of the SHG intensity to excitation power is observed in both MoS_2 and QD/MoS_2 hybrid (Fig. 1d). In striking contrast with the enhancement at only a local hot spot in plasmon- or cavity-related techniques, QD can efficiently boost the SHG of the whole MoS_2 area (Fig. 1e).

The magnitude of SHG enhancement can be tuned by the thickness of QD film (Supplementary Fig. 1), where thicker film leads to larger enhancement and a saturation trend is observed when thickness reaches ~100 nm. Interestingly, the SHG enhancement can be tuned by the interaction distance between QD and MoS_2 as well. Here a SiO_2 spacer layer was inserted between QD and MoS_2 by sequentially depositing SiO_2 layer on MoS_2 monolayer and then coating QD film (Fig. 2a). After the first-step of SiO_2 deposition without QD coating, the SHG intensity of MoS_2 is hardly changed (Supplementary Fig. 2). While after QD coating, SHG is enhanced by ~170 times even under interaction distance R=14 nm (R contains the thickness of SiO_2 layer, the radius of ZnS/CdSe with oleic acid ligand as shown in Fig. 2a) (Fig. 2b). We further systematically monitored the SHG enhancement by tuning the SiO_2 thickness and observed that the increase of interaction distance quickly weakened SHG enhancement with a fitted power coefficient of -2.3 (Fig. 2c). When R reaches ~50 nm, hardly strong SHG enhancement can be observed.

Previously two prevailing scenarios had been proposed to understand the SHG enhancement in 2D materials, i.e. interfacial effects and local-field enhancement. Interfacial effects include charge transfer and symmetry breaking at the interface. Since such high enhancement factor cannot be feasible with the inserted SiO_2 layer, interfacial effect can be first excluded. To verify whether the local-field effect is the origin of such large SHG enhancement in MoS_2, we carefully calculated the SHG response by considering the optical field enhancement of both incident and emitted lights (Supplementary Fig. 3). It turns out that the local-field effect only induces a few times of SHG enhancement with the QD layer coating. We also monitored the two-photon-absorption-induced PL (TPPL) of MoS_2 (its intensity is proportional to the fourth power of the local-field, same as SHG) and observed only several times enhancement with QD coating (Supplementary Fig. 4). We are thus confident to exclude the local-field enhancement as well. Therefore, there must be another mechanism that leads to the giant nonlocal SHG enhancement in MoS_2 by QD coating.

To gain deep insights into the mechanism, we applied wavelength-dependent two-photon excitation measurements. Figure 3a shows the reflective spectra containing the SHG and TPPL of MoS_2 monolayer, QD film and their hybrid under 820 nm pulse laser excitation. These spectra feature sharp peaks at 410 nm and broader peaks at 620 nm, corresponding to SHG signal from MoS_2 and TPPL signal from QD, respectively. As expected, the large two-photon absorption cross section and high PL quantum efficiency render QD high TPPL conversion efficiency up to $\sim 2\times10^{-3}$ (fundamental pump peak intensity of 20 GW/cm^2). Here we note that no detectable TPPL from pristine MoS_2 can be observed under the same condition. After QD coating, the SHG of MoS_2 in the hybrid is enhanced by three orders of magnitude. Meanwhile, the TPPL of QD in the hybrid quenches to ~1/10 of pristine QD film. To catch the relation between SHG enhancement and TPPL quenching (defined as TPPL intensity in QD/MoS_2 to that in pristine QD), we tested ~40 hybrid samples and found that stronger SHG in MoS_2 always accompanies with weaker TPPL in QD (Fig. 3b). This is also consistent with the interaction distance-dependent TPPL of QD in the QD/SiO_2/MoS_2 sandwich hybrid, where the insertion of SiO_2 spacer layer will weaken the SHG enhancement and increase the TPPL intensity at the same time (Supplementary Fig. 5). In the wavelength-dependent two-photon excitation experiments with excitation wavelength tuned from 925 to 720 nm, the TPPL intensity of QD shows continuous increase and a shoulder presents around 820 nm (Fig. 3c). This shoulder is attributed to deep-band states obeying the selection rule of two-photon absorption and hints the strong oscillator strength. In coincidence, the SHG

enhancement in the hybrid also shows a peak at ~820 nm (Fig. 3d). Further controlled experiment in QD/WS_2 hybrid shows that the SHG enhancement of WS_2 presents a peak at ~820 nm as well (Supplementary Fig. 6), although WS_2 has different shape of wavelength-dependent SHG spectra to that of MoS_2. Therefore, the peak in Fig. 3d must stem from the properties of QD rather than the 2D materials. We can safely conclude that the enhancement of SHG in MoS_2 is directly correlated to the strong two-photon absorption and the associated TPPL quenching in QD.

Based on all the above experiments, here we propose a mechanism of nonlinear-excitation resonance energy transfer to understand the greatly enhanced SHG in MoS_2 by QD coating, where second harmonic response dipole in MoS_2 directly gets energy from the two-photon absorption dipole with strong oscillator strength in QD by a high-efficiency remote Coulombic coupling (Fig. 3e)[30]. Generally, the energy transfer rate k^{ET} is determined by two terms, the energy overlap $\int_0^\infty d\varepsilon J(\varepsilon)$ and the Coulombic coupling strength $V_{couping}^{Coul}$, which can be described as

$$k^{ET} = \frac{2\pi}{\hbar}\left|V_{couping}^{Coul}\right|^2 \int_0^\infty d\varepsilon J(\varepsilon), \qquad (1)$$

$$V_{couping}^{Coul} = \frac{e^2}{4\pi\varepsilon_0}\int \frac{P^D(\boldsymbol{r_1})P^A(\boldsymbol{r_2})}{|\boldsymbol{r_1}-\boldsymbol{r_2}|} d\boldsymbol{r_1} d\boldsymbol{r_2}. \qquad (2)$$

Where the energy overlap expresses an overlap between donor emission spectrum $f^D(\varepsilon)$ and acceptor absorption spectrum $f^A(\varepsilon)$, each of which has been normalized to the unit area on energy scale, as $J(\varepsilon) = f^D(\varepsilon)f^A(\varepsilon)$. The Coulombic coupling strength $V_{couping}^{Coul}$ is determined by quantum mechanical oscillator transition densities of donor polarization $P^D(\boldsymbol{r_1})$ and acceptor polarization $P^A(\boldsymbol{r_2})$. Therefore, elaborating donor and acceptor materials for large energy overlap and engineering the coupling strength are two main strategies to get efficient energy transfer.

For traditional linear-excitation energy transfer, such as in fluorescence resonance energy transfer, the donor emission spectrum only overlaps with the side bands of acceptor absorption one, resulting in relatively small values of energy overlap $J(\varepsilon)$. But here for the nonlinear-excitation resonance energy transfer, the two-photon absorption spectrum in QD and SHG of MoS_2 has nearly perfect overlap with each other at any excitation energy, guaranteeing the near-unity $\int_0^\infty d\varepsilon J(\varepsilon)$ (Supplementary Fig. 7). Meanwhile, QD are ideal photoexcited-energy storage materials with generally strong two-photon absorption. Especially under resonant excitation of those deep-band states[10], the strong dipole oscillator strength in QD gives massive stored energy

and strong Coulombic coupling with adjacent MoS_2. These two unique factors in QD together contribute to the high-efficiency energy transfer ($\eta=1-\frac{TPPL_{heterostructure}}{TPPL_{QDs}}$ =95% with QD TPPL quenching of ~0.05) and hence can strengthen the second harmonic response of MoS_2 up to ~1500 times. Under this model, the effective coupling radius, where the energy transfer efficiency drops to 50%, is given as d_0=17 nm. It is worth noting that previous calculation indicating that energy transfer rate should scale as d^{-4} for perfect zero-dimensional (0D)-2D dipole-dipole interaction system. However, in our experiments, the QD have finite size of ~10 nm and also form film structure (~sub-200 nm-thick). This might explain, why our data show the salient feature of $d^{-2.3}$ dependent energy transfer.

Under multiphoton resonant excitation of the deep-band states with strong oscillator strength in QD, our enhancement mechanism is expected to be quite universal for different nonlinear harmonic orders and various 2D forms, as the nonlinear high-order absorption in QD and the same order harmonic generation in 2D materials are always of the same wavelength and have nearly perfect spectral overlap. For example, under 1350 nm excitation, the resonant three-photon absorption in QD and third harmonic generation (THG) in graphene both happen at 450 nm, resulting in the strong THG enhancement in conducting graphene after QD coating (Fig. 4a), via a three-photon-excitation energy transfer process (Inset of Fig. 4a). And the high enhancement is observed in the fourth harmonic generation (FHG) at 390 nm in QD/MoS_2 under excitation at 1560 nm (Fig. 4b). In addition, by coating QD on insulating hBN (Fig. 4c) or organic DANS thin molecular films (Fig. 4d), the SHG signal can also be enhanced, indicating that QD coating is a universal method to enhance the nonlinear optical responses of different 2D materials. We notice that the absolute enhancement factor varies in different nonlinear orders and 2D systems, and currently we don't have a quantitative understanding of this difference. In the near future, more theoretical exploration on the excited dynamics should be carried out and might provide more in-depth information on the nonlinear-excitation resonance energy transfer[39].

In summary, we demonstrated a universal route for spatially homogeneous and giant enhancement on nonlinear optical responses of 2D systems by a high-efficiency remote nonlinear-excitation resonance energy transfer from adjacent QD. The greatly enhanced nonlinear light-matter interactions in 2D materials together with their facile compatibility with current microfabrication technology should open exciting opportunities in the design of optoelectronic and

nanophotonic devices, such as optical communication circuits and frequency upconversion nanolasers.

References

1 Kamat, P. V. Quantum dot solar cells. Semiconductor nanocrystals as light harvesters. *J. Phys. Chem. C* **2008**, 112, 18737-18753.

2 Kim, T.-H., Cho, K.-S., Lee, E. K., Lee, S. J., Chae, J. *et al.* Full-colour quantum dot displays fabricated by transfer printing. *Nat. Photon.* **2011**, 5, 176-182.

3 Qian, L., Zheng, Y., Xue, J.,Holloway, P. H. Stable and efficient quantum-dot light-emitting diodes based on solution-processed multilayer structures. *Nat. Photon.* **2011**, 5, 543-548.

4 Konstantatos, G., Badioli, M., Gaudreau, L., Osmond, J., Bernechea, M. *et al.* Hybrid graphene-quantum dot phototransistors with ultrahigh gain. *Nat. Nanotechnol.* **2012**, 7, 363-368.

5 Shirasaki, Y., Supran, G. J., Bawendi, M. G.,Bulović, V. Emergence of colloidal quantum-dot light-emitting technologies. *Nat. Photon.* **2013**, 7, 13-23.

6 Bao, J.,Bawendi, M. G. A colloidal quantum dot spectrometer. *Nature* **2015**, 523, 67-70.

7 Adinolfi, V.,Sargent, E. H. Photovoltage field-effect transistors. *Nature* **2017**, 542, 324-327.

8 Tang, X., Ackerman, M. M., Chen, M.,Guyot-Sionnest, P. Dual-band infrared imaging using stacked colloidal quantum dot photodiodes. *Nat. Photon.* **2019**, 13, 277-282.

9 Hanifi, D. A., Bronstein, N. D., Koscher, B. A., Nett, Z., Swabeck, J. K. *et al.* Redefining near-unity luminescence in quantum dots with photothermal threshold quantum yield. *Science* **2019**, 363, 1199-1202.

10 Allione, M., Ballester, A., Li, H., Comin, A., Movilla, J. L. *et al.* Two-photon-induced blue shift of core and shell optical transitions in colloidal CdSe/CdS quasi-type II quantum rods. *ACS Nano* **2013**, 7, 2443-2452.

11 Wang, Y., Ta, V. D., Gao, Y., He, T. C., Chen, R. *et al.* Stimulated emission and lasing from CdSe/CdS/ZnS core-multi-shell quantum dots by simultaneous three-photon absorption. *Adv. Mater.* **2014**, 26, 2954-2961.

12 Makarov, N. S., Lau, P. C., Olson, C., Velizhanin, K. A., Solntsev, K. M. *et al.* Two-photon absorption in CdSe colloidal quantum dots compared to organic molecules. *ACS Nano* **2014**, 8, 12572-12586.

13 Wang, Y., Xiao, J., Zhu, H., Li, Y., Alsaid, Y. *et al.* Structural phase transition in monolayer $MoTe_2$ driven by electrostatic doping. *Nature* **2017**, 550, 487-491.

14 Liu, H., Li, Y., You, Y. S., Ghimire, S., Heinz, T. F. *et al.* High-harmonic generation from an atomically thin semiconductor. *Nat. Phys.* **2017**, 13, 262-265.

15 Yoshikawa, N., Tamaya, T.,Tanaka, K. High-harmonic generation in graphene enhanced by elliptically polarized light excitation. *Science* **2017**, 356, 736-738.

16 Sie, E. J., Nyby, C. M., Pemmaraju, C., Park, S. J., Shen, X. *et al.* An ultrafast symmetry switch in a Weyl semimetal. *Nature* **2019**, 565, 61-66.

17 Wu, S., Buckley, S., Schaibley, J. R., Feng, L., Yan, J. *et al.* Monolayer semiconductor nanocavity lasers with ultralow thresholds. *Nature* **2015**, 520, 69-72.

18 Sun, Z., Martinez, A.,Wang, F. Optical modulators with 2D layered materials. *Nat. Photon.* **2016**, 10, 227-238.

19 Yao, B., Huang, S.-W., Liu, Y., Vinod, A. K., Choi, C. *et al.* Gate-tunable frequency combs in graphene–nitride microresonators. *Nature* **2018**, 558, 410-414.

20 Li, Y., Rao, Y., Mak, K. F., You, Y., Wang, S. *et al.* Probing symmetry properties of few-layer MoS_2 and h-BN by optical second-harmonic generation. *Nano Lett.* **2013**, 13, 3329-3333.

21 Cheng, J.-L., Vermeulen, N.,Sipe, J. Third order optical nonlinearity of graphene. *New Journal of Physics* **2014**,

16, 053014.

22 Seyler, K. L., Schaibley, J. R., Gong, P., Rivera, P., Jones, A. M. *et al.* Electrical control of second-harmonic generation in a WSe_2 monolayer transistor. *Nat. Nanotechnol.* **2015**, 10, 407-411.

23 Liang, J., Zhang, J., Li, Z., Hong, H., Wang, J. *et al.* Monitoring local strain vector in atomic-layered $MoSe_2$ by second-harmonic generation. *Nano Lett.* **2017**, 17, 7539-7543.

24 Jiang, T., Huang, D., Cheng, J., Fan, X., Zhang, Z. *et al.* Gate-tunable third-order nonlinear optical response of massless Dirac fermions in graphene. *Nat. Photon.* **2018**, 12, 430-436.

25 Soavi, G., Wang, G., Rostami, H., Purdie, D. G., De Fazio, D. *et al.* Broadband, electrically tunable third-harmonic generation in graphene. *Nat. Nanotechnol.* **2018**, 13, 583-588.

26 Aouani, H., Rahmani, M., Navarro-Cia, M.,Maier, S. A. Third-harmonic-upconversion enhancement from a single semiconductor nanoparticle coupled to a plasmonic antenna. *Nat. Nanotechnol.* **2014**, 9, 290-294.

27 Lee, J., Tymchenko, M., Argyropoulos, C., Chen, P.-Y., Lu, F. *et al.* Giant nonlinear response from plasmonic metasurfaces coupled to intersubband transitions. *Nature* **2014**, 511, 65-69.

28 Wen, X., Xu, W., Zhao, W., Khurgin, J. B.,Xiong, Q. Plasmonic hot carriers-controlled second harmonic generation in WSe_2 bilayers. *Nano Lett.* **2018**, 18, 1686-1692.

29 Shi, J., Li, Y., Kang, M., He, X., Halas, N. J. *et al.* Efficient second harmonic generation in a hybrid plasmonic waveguide by mode interactions. *Nano Lett.* **2019**, 19, 3838-3845.

30 Scholes, G. D. Long-range resonance energy transfer in molecular systems. *Annu. Rev. Phys. Chem.* **2003**, 54, 57-87.

31 Hernández-Martínez, P. L., Govorov, A. O.,Demir, H. V. Generalized theory of Förster-type nonradiative energy transfer in nanostructures with mixed dimensionality. *J. Phys. Chem. C* **2013**, 117, 10203-10212.

32 Cox, J. D.,Garcia de Abajo, F. J. Nonlinear atom-plasmon interactions enabled by nanostructured graphene. *Phys. Rev. Lett.* **2018**, 121, 257403.

33 Achermann, M., Petruska, M. A., Kos, S., Smith, D. L., Koleske, D. D. *et al.* Energy-transfer pumping of semiconductor nanocrystals using an epitaxial quantum well. *Nature* **2004**, 429, 642-646.

34 Tisdale, W. A., Williams, K. J., Timp, B. A., Norris, D. J., Aydil, E. S. *et al.* Hot-electron transfer from semiconductor nanocrystals. *Science* **2010**, 328, 1543-1547.

35 Gaudreau, L., Tielrooij, K. J., Prawiroatmodjo, G. E., Osmond, J., Garcia de Abajo, F. J. *et al.* Universal distance-scaling of nonradiative energy transfer to graphene. *Nano Lett.* **2013**, 13, 2030-2035.

36 Rowland, C. E., Fedin, I., Zhang, H., Gray, S. K., Govorov, A. O. *et al.* Picosecond energy transfer and multiexciton transfer outpaces Auger recombination in binary CdSe nanoplatelet solids. *Nat. Mater.* **2015**, 14, 484-489.

37 Raja, A., Montoya Castillo, A., Zultak, J., Zhang, X. X., Ye, Z. *et al.* Energy transfer from quantum dots to graphene and MoS_2: the role of absorption and screening in two-dimensional materials. *Nano Lett.* **2016**, 16, 2328-2333.

38 Zhu, X., Monahan, N. R., Gong, Z., Zhu, H., Williams, K. W. *et al.* Charge transfer excitons at van der Waals interfaces. *J. Am. Chem. Soc.* **2015**, 137, 8313-8320.

39 Engelmann, A., Yudson, V.,Reineker, P. Enhanced optical nonlinearity of hybrid excitons in an inorganic semiconducting quantum dot covered by an organic layer. *Phys. Rev. B* **1998**, 57, 1784.

Acknowledgements: This work was supported by National Natural Science Foundation of China (52025023, 52021006, 51991340, 51991342, 51722204, 51972041, 51972042, 51672007 and 11974023), the National Key R&D Program of China (2016YFA0300903 and 2016YFA0300804), Beijing Natural Science Foundation (JQ19004), Beijing Excellent Talents Training Support (2017000026833ZK11), the Strategic Priority Research Program of Chinese Academy of Sciences (XDB33000000), Beijing Municipal Science & Technology Commission (Z191100007219005), Beijing Graphene Innovation Program (Z181100004818003), Key-Area Research and Development Program of GuangDong Province (2020B010189001, 2019B010931001, and 2018B030327001), Guangdong Innovative and Entrepreneurial Research Team Program (2016ZT06D348), the Science, Technology and Innovation Commission of Shenzhen Municipality (KYTDPT20181011104202253), Bureau of Industry and Information Technology of Shenzhen (Graphene platform 201901161512), Beijing Municipal Science & Technology Commission (Z191100007219005), National Equipment Program of China (ZDYZ2015-1) and the China Postdoctoral Science Foundation (2020M680177).

Author contributions: K.L. designed the experiments. K.L. and J.X. supervised the project. H.H., C.W. and Z.Z. performed the frequency harmonic generation experiments. F.W., J.F., H.S., and Y.W. provided the QD samples. Y.Z., J.W., C.L. and Y.Z. grew MoS_2 and WS_2 samples. J.Z., J.Y., K.L., P.G., S.M., S.W. and Z.S. suggested the optical experiments. K.L. and H.H. wrote the manuscript. All authors contributed to the scientific discussion and modifying the manuscript.

Methods:

Synthesis of CdSe/ZnS core/shell colloidal QD. A mixture of Se (0.158 g, 2 mmol), octadecylamine (ODA) (1.62g, 6mmol), and 20 mL of 1-octadecene (ODE, 90%) was heated to 120 ℃ for 30 min, and then to 220 ℃ for 4 h to prepare Se precursor. A mixture of ZnO (0.326 g, 4 mmol), oleic acid (5.64 g, 16 mmol), and ODE (13.7 mL) was heated to 310 ℃ to prepare the zinc solution precursor. CdO (0.0154 g, 0.12 mmol), stearic acid (0.36 mmol), and ODE were mixed and heated to 280 ℃ under nitrogen flow. Then 2 mL prepared Se precursor was injected.

When the color tune to dark red, the mixture was cooled down to room temperature and the CdSe nanocrystals were prepared. The as-prepared CdSe nanocrystals were firstly purified by repeated precipitation with methanol for several times and then dispersion in hexanes. 3 mL of ODE, 1 g of ODA and the purified CdSe core in hexanes were mixed at 100 ℃ under nitrogen flow for 20 min to remove hexanes. Subsequently, the solution was heated to 180~280 ℃ for the shells growth. The linear absorption and PL spectra of CdSe/ZnS QD with band gap of 620 nm used in our experiments are shown in Supplementary Fig. 8.

Fabrication of QD hybrid. Triangle shape MoS_2 monolayer was grown on SiO_2/Si substrate through chemical vapor deposition process using MoO_3 and S powder as precursors at atmospheric pressure. hBN monolayer was grown on copper foil and then transferred to SiO_2/Si substrate. Graphene monolayer was exfoliated on fused silica. DANS molecule was spin coating on SiO_2/Si substrate. Then CdSe/ZnS core/shell QD film was deposited on MoS_2, hBN, graphene or DANS by spin coating. The thickness of QD film on each 2D material can be controlled by the QD solution concentration and the spin coating conditions. For different 2D materials, the QD coating thicknesses can be different.

Harmonic generation measurements. Two systems were alternatively used in our harmonic generation measurement. Wavelength-dependent SHG was excited by Spectra-Physics Mai Tai oscillator (~100 fs, 80 MHz, 690-1050 nm). THG and FHG were excited by Coherent Vitara-T oscillator and optical parametric amplifier (OPA) 9850 laser system (~70 fs, 250 kHz, 1200-1600 nm). Excitation laser was focused by a Nikon objective (60X, NA=0.65) and the harmonic generation signal was collected by the same objective with reflection mode. After filtering out the excitation laser, the harmonic generation signal was recorded by a Princeton SP2500 spectrometer equipped with a nitrogen-cooled Si charge coupled device (CCD). For the polarization-dependent SHG pattern, we recorded the SHG with polarization parallel to that of excitation laser. The experimental scheme is shown in our previous work[23]. All our experiments were done at room temperature.

Figures and captions

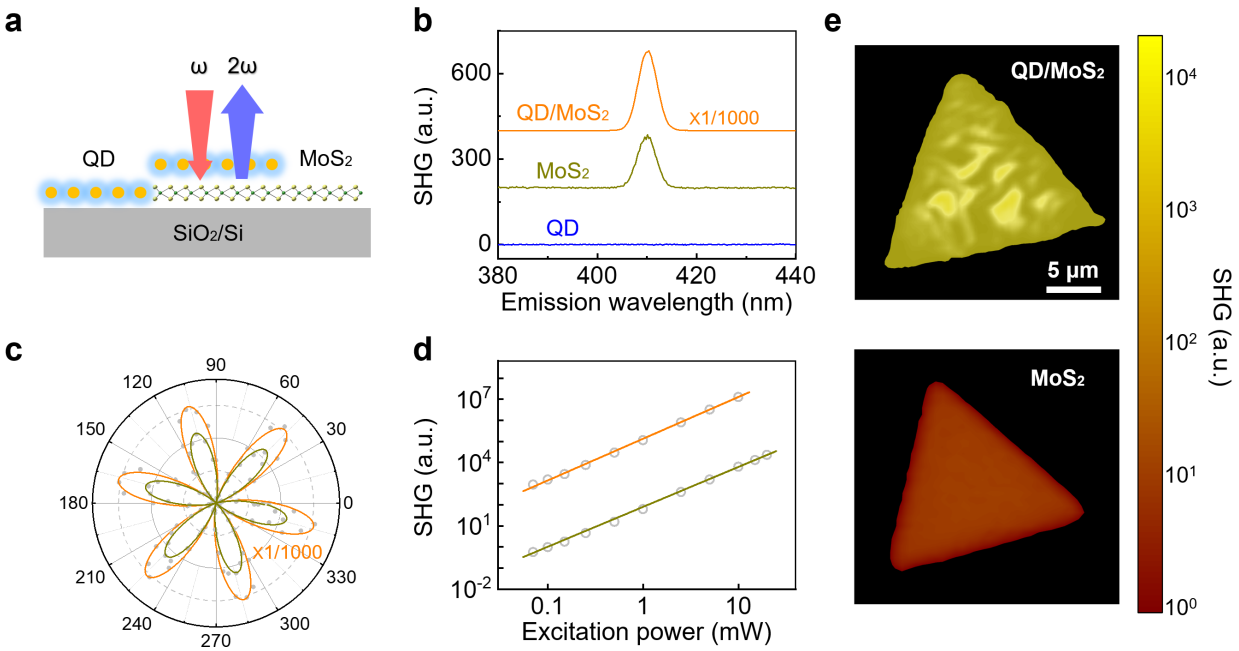

Figure 1 | MoS_2 monolayer SHG enhancement with QD coated. a, Side-view illustration of QD/MoS_2 hybrid structure and its optical SHG. **b**, SHG spectra of MoS_2 and QD/MoS_2 under 820 nm pulse laser excitation. With QD decorating, the weak SHG of MoS_2 can be boosted by ~1500 times in the hybrid. For comparison, no apparent SHG signal can be observed in pristine QD. **c**, Polarization-dependent SHG patterns measured on a MoS_2 monolayer and its QD hybrid. **d**, Excitation power dependence of SHG peak intensity for MoS_2 and QD/MoS_2 hybrid, where both curves show the expected quadratic law. **e**, Spatial SHG intensity mapping images of a MoS_2 monolayer before (bottom) and after (up) QD coating.

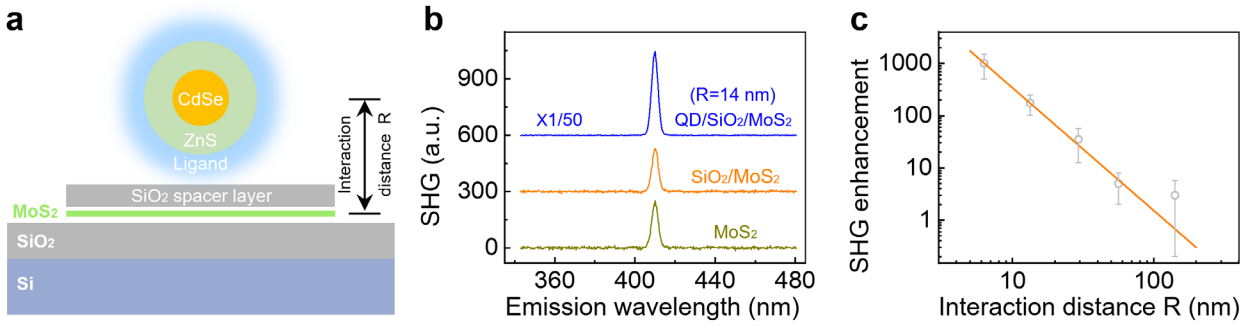

Figure 2. Interaction distance-dependent SHG enhancement. a, Schematic illustration of fabricated QD/SiO_2/MoS_2 sandwich hybrid structure by sequentially depositing SiO_2 and QD on MoS_2. The interaction distance R between MoS_2 and QD film can be systematically tuned by the thickness of the SiO_2 spacer layer. **b**, SHG spectra of MoS_2 and fabricated hybrid structures. With interaction distance of ~14 nm, SHG intensity of MoS_2 can still be enhanced by ~170 times. For comparison, without QD, SiO_2 layer hardly influences the SHG intensity. **c**, Interaction distance-dependent SHG enhancement. Increase of interlayer distance quickly weakens the SHG enhancement with a fitted power coefficient of -2.3. The error bar is standard deviation measured from 10 samples.

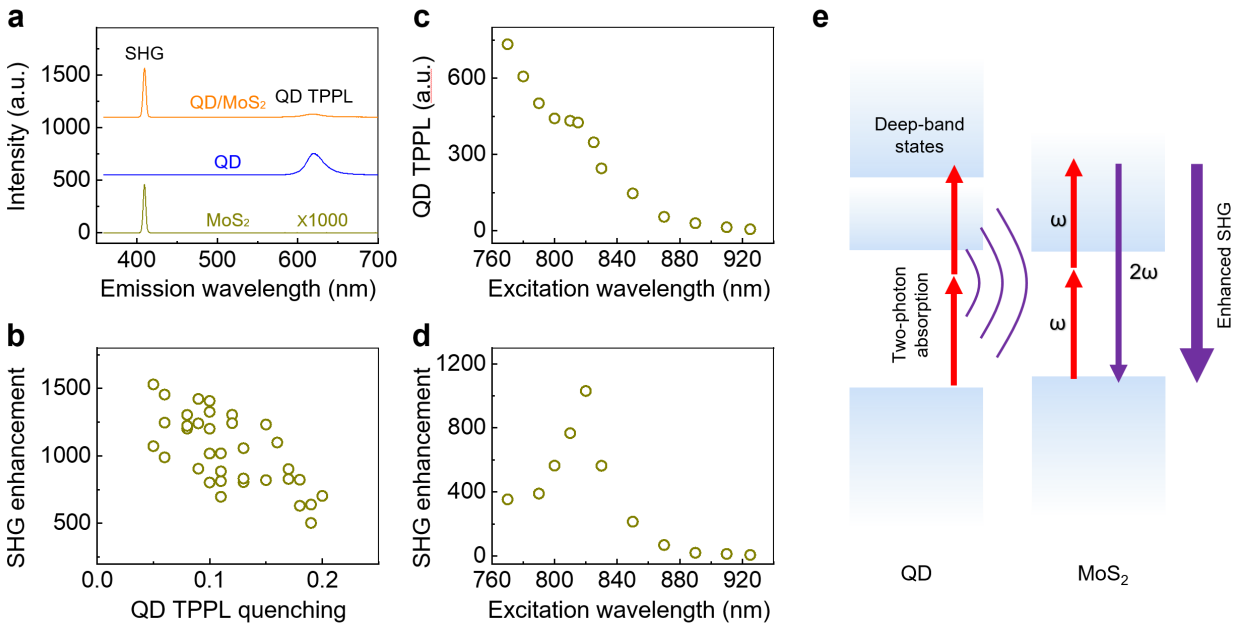

Figure 3. Excitation wavelength-dependent SHG enhancement. a, SHG and TPPL spectra of pristine MoS_2 monolayer, QD film and their hybrid under excitation of 820 nm pulse laser. The sharp peak at 410 nm is the SHG of MoS_2 and the broader peak at 620 nm corresponds to TPPL of QD. Compared with its component layers, the QD/MoS_2 hybrid shows enhanced MoS_2 SHG and quenched QD TPPL. **b**, The MoS_2 SHG enhancement versus QD TPPL quenching in the hybrid structure obtained from ~40 samples. With SHG enhanced more strikingly, the QD TPPL quenched more significantly. **c-d**, Wavelength-dependent TPPL of pristine QD film (c) and SHG enhancement in the QD/MoS_2 hybrid (d) under two-photon excitation. TPPL spectrum of QD presents a shoulder around ~820 nm, indicating the existence of deep-band excited states with strong oscillator strength and high two-photon absorption. In coincidence, the SHG enhancement in the hybrid shows a peak at ~820 nm as well. **e**, Scheme of nonlinear-excitation resonance energy transfer and SHG enhancement. Under resonant excitation of the deep-band two-photon excited states in QD, strong dipole coupling and perfect energy overlap between QD and MoS_2 facilitate the high-efficiency energy transfer and hence substantially strengthen the second harmonic response.

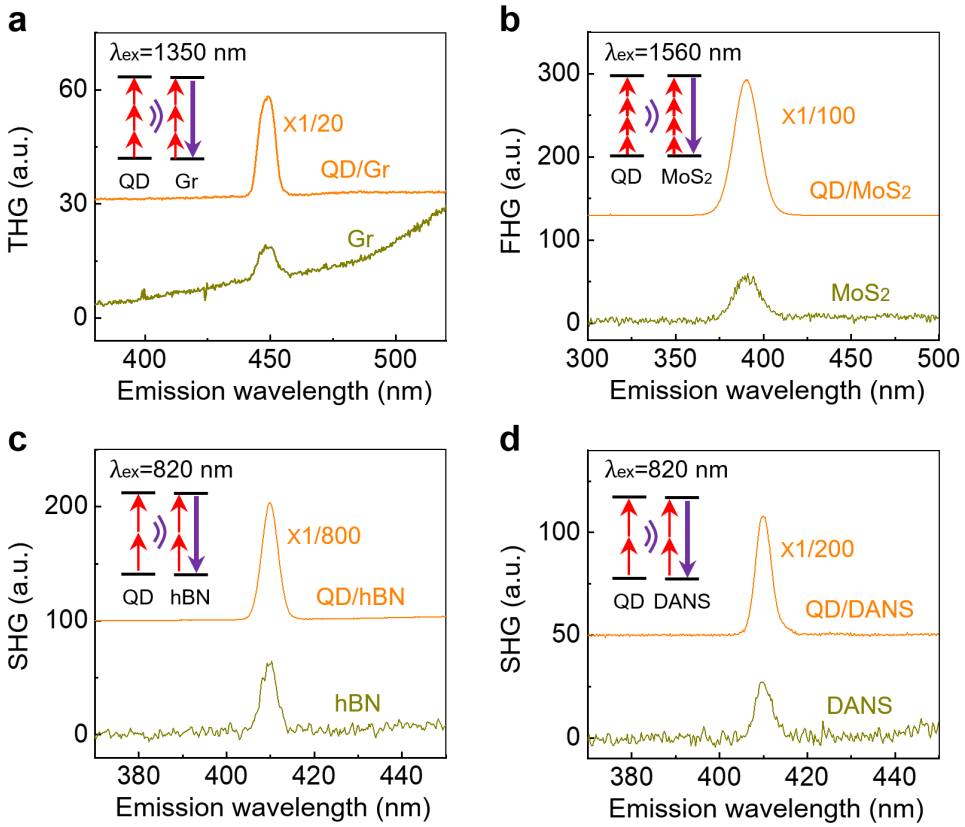

Figure 4. Universal optical nonlinearity enhancement of various 2D systems with different frequency harmonic orders. a, b, Higher frequency harmonic orders enhancement. After QD coating, both the third harmonic generation (THG) of conducting graphene under excitation of 1350 nm (a) and the fourth harmonic generation (FHG) of semiconducting MoS_2 under excitation of 1560 nm (b) are enhanced. **c, d,** Optical nonlinearity enhancement of various 2D systems. Beside the conducting graphene and semiconducting MoS_2, QD coating can also enhance the SHG of insulating hBN (c) and DANS thin molecular films (d). The excitation wavelength for SHG is 820 nm. The insets schematically illustrate the nonlinear-excitation resonance energy transfer from QD to 2D materials for optical nonlinearity enhancement.